Impact of Iron Oxide Nanoparticles Additives in Water Hyacinth/Diesel Biofuel Mixture on CI Engine Performance and Emissions

Ahmed Fadhil[1], Alaa Dhari Jawad Al-Bayati[2], Hasanain A. Abdul Wahhab[3*]

[1] Power Technical Engineering Department, Al-Amarah University College, Amarah 35115, Iraq
[2] Chemical Engineering Department, Al-Mustaqbal University College, Hilla 35088, Iraq
[3] Training and Workshop Center, University of Technology- Iraq, Baghdad 35050, Iraq

Corresponding Author Email: 20085@uotechnology.edu.iq

This article is part of the Special Issue Ajman 6th International Environment Conference

ABSTRACT

The integration of diesel and biodiesel, particularly biodiesel derived from water hyacinth, as a combined fuel source has recently emerged as a promising area of study, with a particular focus on the effects of nanoparticle additives. Notably, the reduction of emissions achieved by introducing iron oxide nanoparticles (Fe_3O_4) to biodiesel has been substantiated. However, the potential impact of blending nanoparticles with the diesel and biodiesel mix on the performance characteristics of a diesel engine has yet to be sufficiently explored. This research undertook performance and emission assessments employing diverse fuel samples in a single-cylinder diesel engine. The thermal brake efficiency metrics for the 50 ppm and 100 ppm iron oxide nanoparticle blends surpassed those of the D80B20 and D60B40 biofuel blends, exhibiting increases of 3.5% and 4.85% for D80B20N50 and D80B20N100, and 6.2% and 7.4% for D80B20N50 and D80B20N100, respectively, in comparison to neat diesel. The carbon monoxide emission levels of the biofuel blends with iron oxide were less than that of neat diesel, with the most significant reduction detected in the D60B40N100 blend. Furthermore, the nitrogen oxide emissions for all nanoparticle blends were lower than those for neat diesel, attributable to a shortened ignition delay and minimized fuel usage during combustion, subsequently leading to a reduction in nitrogen oxide emissions.

1. INTRODUCTION

Consumption of the product of petroleum is growing every day as vehicle numbers are growing, resulting in large-scale consumption of hydrocarbon fuel, which worsens environmental pollution. Therefore, such two problems, fuel supply and ecological contamination require urgent solutions [1-3]. Non-renewable fuel emits further emissions of hydrocarbon, nitrogen oxides, and monoxides of carbon and sulfur when in comparison with renewable biofuels. Different substituted fuels have been proposed, like alternates for petroleum products, and attempts have been made to analyze their viability. Renewable fuels have recently received great attention for their potential to reduce environmental pollution by completing the carbon cycle and reducing petroleum imports [4-6]. Also, there has been a considerable attempt in numerous developing states worldwide to extract ethanol from the water hyacinth owing to its richness as well as the high yield of biomass. For instance, in India, the investigators have obtained the bio-conversion approaches of extracting bioethanol from the plant through enzymes and diluting sulphuric acid beneath elevated pressure and temperature [7, 8].

Increasing efficacy and decreasing diesel engine emissions are the chief goals of numerous current pieces of research. One way of doing so is by using nanoparticles as fuel additives [9, 10], which shows a significant rise in combustion quality and, therefore, in the engine's overall performance [11-13]. Many researchers have investigated the impact of different oxygenated additions on biofuels for enhancing the combustion and emission features of internal combustion engines. And for example, the engine's combustion and performance features were improved by adding nanoparticles of metallic oxides to fuel mixes since such a supplement raises the thermal efficacy and the heat release rate [14, 15]. To elaborate further, the benefits of metal-oxide nanoparticle additives include the capability to donate the atoms of oxygen to the mix of utilized fuel and create an elevated ratio of surface-to-volume. Thus, these nanoparticle additives act as a highly reactive medium throughout combustion.

Furthermore, the nanoparticle addition raises the thermal conductivity, fire-point, and flashpoint temperature, reducing the kinematic viscosity [16]. Ashoka et al. [17] investigated the potential of Pentanol (10, 20, and 30%) as a low reactivity fuel, which is a cetane value improver. Jatropha oil blended with diesel is considered the high reactivity fuel. Results show that Pentanol affects emission and combustion properties [18]. It also plays a key role in developing performance characteristics such as fuel development technologies. The increasing demand to improve the diesel engine's performance leads to opening the way for better investment in biofuel

sources through the use of additives such as nanomaterials. In recent studies, the effect of nano additives at different concentrations was tested with diesel and biodiesel (0 to 50 %) to determine diesel engine performance in terms of specific brake fuel consumption, brake power, and thermal efficiency under different conditions [19, 20]. Engine emissions are mainly classified into two different categories, the first is produced because of high combustion chamber temperature, such as nitrogen oxides, and the second is caused by incomplete combustion of fuels and low combustion temperatures, such as hydrocarbon and carbon dioxide. Many researchers discussed an enhanced protocol to produce new biodiesel using palm crude oil when using alkali-catalyzed trans-esterification, using the nonedible solid portion of palm oil [21]. Carbon monoxide is produced due to incomplete combustion, a reduction in the combustion time of the engine, or a decrease in the temperature of the combustion chamber [22, 23]. On the other hand, incomplete combustion of diesel or fuel will result in the production of hydrocarbons. Soot is caused by the incomplete combustion of hydrocarbon fuels and is observed in dark exhaust tailings.

In recent years, millions of dollars have been spent yearly to remove large masses of water hyacinth, inhibiting water flow in Iraqi rivers. The water hyacinth plant's quantitative statistics extracted via the Aquatic Treatment Directorate depict that the plant will cover around (950 km^2) in 2021 in the south of Iraq. Water hyacinth plants can be used for producing biodiesel or as an alternative to diesel fuel. The main objectives of the present study are to analyze the complex information, determine the diesel-biodiesel (from water hyacinth) blends' effects on the performance characteristics and the exhaust emissions of the diesel engine, as well as develop further understanding of the biofuel blend after improving it by blending it with iron oxide, Fe_3O_4 nanoparticles.

2. EXPERIMENTAL SETUP

2.1 Preparation of test samples blends

Experimentally, biofuel ethanol has been made in several stages. First, the roots, leaves, and petioles have been detached from the water hyacinth plant, and the leaves and petioles have been washed manually with tap water. Second, a plant specimen was dried in an oven, and the dried material was ground to powder. Then, they were pretreated with 1.0% NaOH for 2 hours. Third, 10 kg of water hyacinth with a 6.0 wt. % of sulphuric acid catalysts with a 5:1 methanol-to-oil ratio of 5:1 was treated in a hydrodynamic cavitation reactor at 65°C utilizing circulating glycerin for 45 min. A 50 L capacity has been employed for producing the water hyacinth-oil biodiesel. Two samples have been prepared for the present investigations. D80B20 has been extracted from 20% water hyacinth biofuel, with 80% neat diesel based on volume and D60B40. The specifications of the three blends are shown in Table 1.

Table 1. Properties of the test samples used in the experiments

	D	D80B20N50	D80B20N100	D60B40N50	B60B40N100
Density, kg/m^3	825	831.5	831.9	842.3	842.8
Viscosity, cSt	2.2	3.18	3.2	3.41	3.44
Cetane No.	52.8	50.3	49.8	47.4	47.1
Calorific value, kcal/kg	10290	10267	10270	10253	10260
Cloud point, °C	< - 21.2	- 21.3	- 21	- 21	- 21
Flashpoint, °C	61	-	-	-	-

Nano mixtures have been produced individually by biodiesel blend D80B20, removed from 20% water hyacinth biofuel with 80% neat diesel, and D60B40, extracted from 40% water hyacinth biofuel with 60% neat diesel, with Fe_3O_4 nanoparticles at a 50 ppm dosage of 100 ppm of mass fraction with an ultrasonicate aid. The nanoparticles were weighed to 50 ppm and dispersed in biodiesel mixtures with ultrasonication's help. The ultrasonic processor is a JP-4820 model with 60 W power and 40 kHz for 30 min frequency for generating nanoparticles-blended biodiesel fuel (D80B20+50 ppm. The same procedure has been attempted for a 100 ppm mass portion. Then, such samples were utilized in the setup of diesel engines to study their performance and emission features. The physic-chemical properties of the whole samples of fuel considered (D80B20N50, D80B20N100, D60B40N50, and B80B40N100) for all nanoparticle samples have been measured according to the ASTM standards, and the outcomes are presented in Table 1. The fuel samples were placed in test tubes in stable conditions to evaluate the stability properties. Through the characterization tests, it was found that they were stable for more than a month.

2.2 Engine specifications and apparatus

Experiments have been conducted employing a 4-stroke CI

Diesel engine single cylinder depicted in Figure 1 with a group of measuring instruments and a gas analyzer. The Diesel CI engine operates upon the opinion of straight as well as natural injection of fuel. It possesses design characteristics with a 70 mm bore of the cylinder, a 55 mm stroke, and a 17:1 compression ratio. Table 2 lists the specifications of the engine. Some investigational characteristics have been gathered: Speed of the engine, the volume rate of fuel flow, the rate of the mass flow of air, and output power (load of engine). An orifice regime has been utilized for measuring the air flowing's quantity inside the engine by erecting it into the box of air. Also, the pressure difference has been registered employing a manometer, whereas the engine's speed has been registered utilizing a digital tachometer. The consumed fuel has also been measured employing a constant size and a stopwatch. BEA 460 Bosch gas analyzer has been utilized to record exhaust emissions.

Additionally, acquisition software provided by Bosch has been implemented as a system of data acquisition as well as process control. The whole test has been achieved for a fixed speed of the engine at the various loads of the engine. Every functional examination took 3-5 min until the stabilization of the engine beneath steady circumstances.

Figure 1. Experimental Diesel engine setup

Table 2. Specifications of tested engine

Engine Model	Loben-RB170F
Engine Type	Four-stroke single
The Bore	70 mm
The Stroke	55 mm
The Displacement	0.221 L
Ratio of Compression	17:1
Speed of Engine	3000 - 3600 rpm
System of Cooling	Air-cooled system
Fuel Injection	Direct injection

2.3 Uncertainty analysis

The analysis of uncertainty analysis in tests is crucial for providing a high level of confidence in the whole outcomes. It is obtained via obtaining repeatability and raising the outcomes' importance. The tests were repeated three times. Also, the variations of the forecast values of the performance parameters and the exhaust emissions have been employed for calculating the uncertainty utilizing the percentage relative standard error, Φ, as shown in Eq. (1) [24]:

$$\Phi\% = \left(\frac{S}{Y}\right) \times 100 \tag{1}$$

where, S is the standard error; Y is the mean of gathered data. Eq. (2) computes the value of S as:

$$S = \frac{\alpha}{\sqrt{k}} \tag{2}$$

where, α is the standard deviation, and k is the repeatable readings of the performance, combustion features, and emission parameters. The overall investigational uncertainty (α_n) is computed by Eq. (3):

$$\alpha_n = \sqrt{\alpha_1^2 + \alpha_2^2 + \cdots + \alpha_i^2} \tag{3}$$

where, α_n is the total uncertainty, and α_1, α_2, and α_i are the uncertainties of the individual factors. The accuracies and the uncertainties of the measured factors are revealed in Table 3.

Table 3. Uncertainties of the measured parameters

Parameter	Max. Value	Accuracy	Uncertainty
Power (kW)	2.1	±0.08 kW	±0.76
Speed (rpm)	3000	±1rpm	±1.85
BSFC (g/kWh)	512	±1.91g/kWh	±0.97
CO (Vol %)	23.7%	±0.03 Vol %	±1.76
HC (ppm)	57	±2 ppm	±1.89
NOx (ppm)	1110	±2 ppm	±3.45

3. RESULTS AND DISCUSSION

Brake thermal efficacy, η_b variation with the engine load for all tested blends D, D80B20N50, D80B20N100, D60B40N50, and D60B40N100 is manifested in Figure 2. The brake thermal efficiency of all fuel blends increased with the increase in load up to full load. In contrast, neat diesel (D) increased with the load up to 90% of the full loading condition. It then started decreasing due to oxygen in biodiesel, which improved the brake thermal efficiency and increased the heat release rate. While the iron oxide nanoparticles 50 ppm, 100 ppm, and biodiesel blends were higher than biofuel D80B20 and D60B40 blends, they increased by 3.5% and 4.85% for D80B20N50 and D80B20N100, respectively, leading to another increase of 6.2% and 7.4% for D80B20N50 and D80B20N100, respectively, when compared to neat diesel. These results agree with the inferences of different research [25-27].
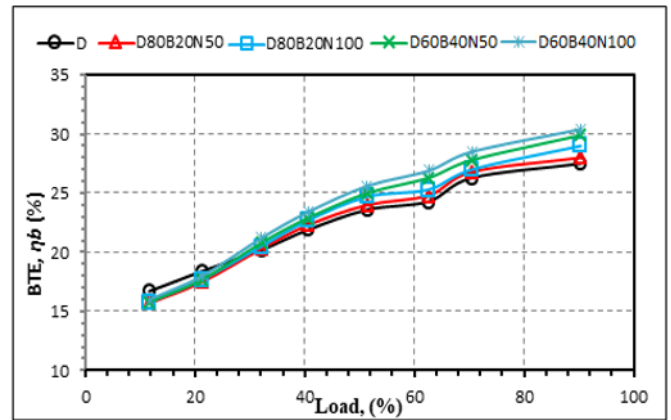

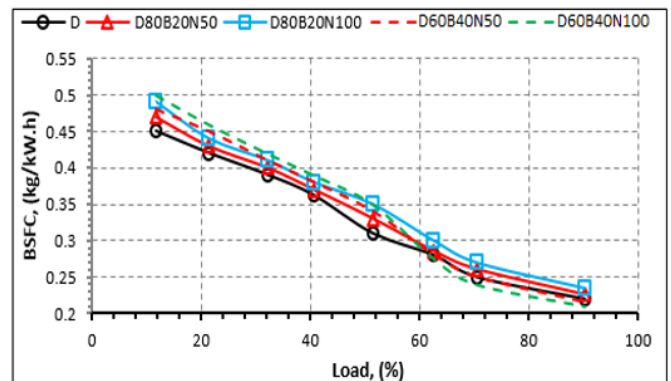**Figure 2.** Brake thermal efficacy variation with the engine load at various mixes of fuel

Figure 3. BSFC Variation with the load of the engine at various mixes of fuel

Brake-Specific Fuel Consumption (BSFC) variation with a load of the engine is manifested in Figure 3 for the neat diesel and the biodiesel mixes with the iron oxide nanoparticles 50 and 100 ppm D, D80B20N50, D80B20N100, D60B40N50, and D60B40N100, which determines the fuel mass that consumed in the unit power output. It was revealed that for the whole test of fuel, the BSFC decreased as the engine load increased, improving the combustion process. Also, biodiesel blends with nanoparticles showed more fuel consumption for the whole conditions than diesel because of the lower heating value and higher density of the blends. This result agrees with the conclusions of various research works [6, 9]. Then the BSFC changed to decrease at a load near the full load. For the D60B40N100, the brake-specific fuel consumption increased by 11.45% at low loads and decreased at a load near the full load compared to neat diesel. It decreased by about 12.9% at full load because of the efficient burning of biodiesel blend with the nanoadditives at higher loading circumstances. This increase in blends BSFC is attributed to the biodiesel's higher density and lower heating value. BSFC differences between the diesel fuel and biodiesel blends were reduced at supercharged conditions.

Figure 4 illustrates the variations of the emission of the CO of the diesel fuel (D), a mix of diesel as well as biodiesel, and iron oxide nanoparticles D80B20N50, D80B20N100, D60B40N50, and D60B40N100 at various engine loads. Generally, CO emissions occur due to fuel-rich combustion and insufficient time. The CO emissions were assessed at various loading circumstances of the tested engine, changing from a load of 10% to a close full load of 90%. The outcomes elucidated that CO emissions rise with the engine's load since CO emissions are very reliant upon the ratio of air/fuel.
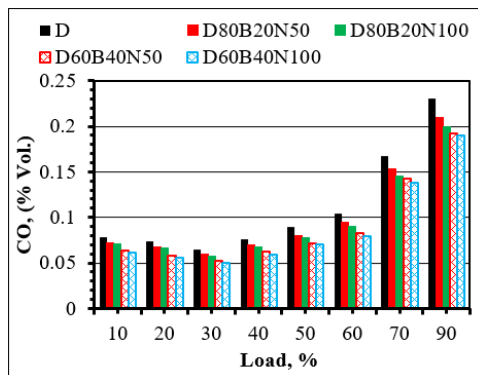

Figure 4. Emission of the CO variation for the tested fuel mix samples at different engine loads

Also, the findings showed that the emission of CO decreased in D80B20N50, D80B20N100, D60B40N50, and D60B40N100 in the whole loading circumstances. For the CO emissions shown in Figure 4, biodiesel blends produced lower CO emissions than neat diesel. This results from a higher oxygen element in the biodiesel fuels, enhancing the combustion process. Higher oxygen content ensured complete combustion by allowing more carbon to burn. In contrast, the higher cetane number for diesel ensured higher flame speed and post-flame oxidation, prolonging the combustion duration and reducing the possible formation of a rich fuel zone. Such influence is obvious through the close full circumstances of loading but isn't too vigorous at the lower loads due to their lower values. Additionally, the emissions rates of CO for both biodiesel and Fe_3O_4 blends were lower than that for the pure

diesel at the whole load circumstances. The best reduction was observed for the D60B40N100 blend, which was about 8.3% compared to the neat diesel owing to the greater thermal conductivity for Fe_3O_4 nanoparticles and higher surface area for catalytic activity [28].

The presence of unburned hydrocarbons in exhaust gases is one of the most important parameters for studying emission characteristics. The changing of unburnt hydrocarbons with the engine load for all tested fuel samples D, D80B20N50, D80B20N100, D60B40N50, and D60B40N100 are given in Figure 5. The HC emissions level for the pure diesel fuel and the biodiesel blend with nano D80B20N50 and D80B20N100 are 58 ppm and 54.22 ppm, respectively, at a load near full load, while the lowering of about 7.9% and 6.9% was due to the higher oxygen concentration in the air-fuel mixture, which can help enhance the unburnt oxidation hydrocarbon. HC emissions decreased with increasing biodiesel percentage in the blend [15]. Also, Figure 5 indicates the change of unburned hydrocarbons (HC) with the engine load for the nanoparticle blends D60B40N50 and D60B40N100. The HC emissions decreased at all load conditions for the biodiesel, and Fe_3O_4 blends D80B20N50 and D80B20N100. This change is due to the increased flame propagation velocity and the higher level of post-flame oxidation from the higher number of cetane in the biodiesel mixture, which ensures the extra quality of combustion [15].
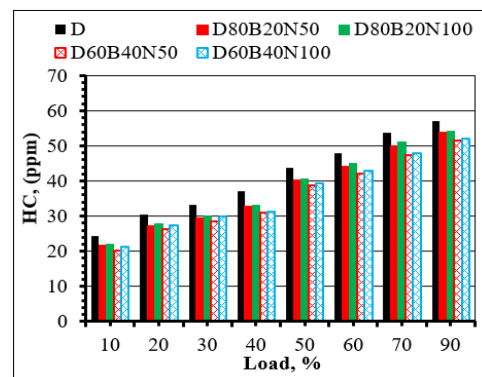

Figure 5. HC emission variation for the tested fuel mix samples at different engine loads
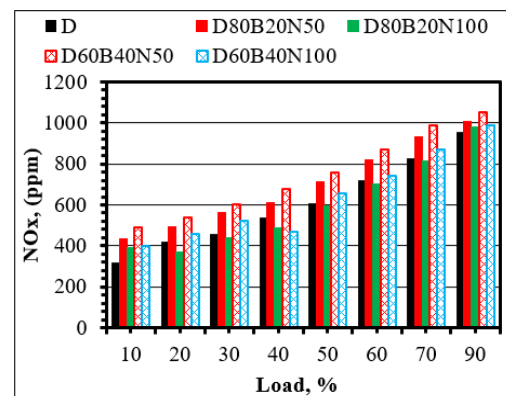

Figure 6. Emission of NOx variation for the tested fuel mix samples at different engine loads

The emission of NOx is related to the oxidation of nitrogen at high temperatures. The variation of the NO emissions with the engine load for all tested fuels - D, D80B20N50, D80B20N100, D60B40N50, and D60B40N100 is given in

Figure 6. Compared with neat diesel fuel, the NO emission increased by about 11.9% and 8.9% for the biodiesel blends with Nano, D80B20N50, and D80B20N100, respectively, at near full load conditions, while the NO emission increased by about 13.9% and 10.8%, respectively, for samples D60B40N50 and D60B40N100. Biodiesel fuels showed significantly higher NO emissions in comparison to diesel fuel. This resulted from a shorter ignition delay period, large spray droplet size, and high adiabatic flame temperature. Factors such as a higher carbon double bond also increase the free radical's hydrocarbon formation and NO emission formation. The high temperatures of combustion break down the vigorous triple bond of the molecules of N_2, disassociate these molecules into their atomic conditions, contribute to a reaction sequence with O_2, and create thermal NOx [16, 21]. Moreover, for the blends with Fe_3O_4 nanoparticles, the NOx emissions were lower than that for biodiesel blend to neat diesel due to shortened ignition delay and less fuel during combustion [16].

4. CONCLUSIONS

Biodiesel and Fe_3O_4 nanoadditives to neat Diesel mixtures have been investigated to evaluate the emissions reduction. Operating under the tested mixtures, the engine performance has also been measured. The physic-chemical properties of the produced fuel samples are measured per the ASTM standards. The subsequent conclusions could be drawn:

-The brake thermal efficiency for the iron oxide nanoparticles with 50 ppm, 100 ppm, and biodiesel blends was higher than the biofuel blends D80B20 and D60B40. It increased by 3.5% and 4.85% for D80B20N50 and D80B20N100, respectively, while it increased by 6.2% and 7.4% for D80B20N50 and D80B20N100, respectively, in comparison with pure diesel.

-CO emission increased with the engine's load. In all loading conditions, CO emission was decreased in D80B20N50 and D80B20N100 fuel, including D60B40N50 and D60B40N100.

-Compared to neat diesel fuel, the NO emission increased by about 11.9% and 8.9% for the biodiesel blends with Nano, D80B20N50, respectively. The NO emission increased by about 13.9% and 10.8%, respectively, for samples D60B40N50 and D60B40N100.

REFERENCES

[1] Abdul Wahhab, H.A., Al-Kayiem, H.H. (2021). Environmental risk mitigation by biodiesel blending from eichhornia crassipes: Performance and emission assessment. Sustainability, 13(15): 8274. https://doi.org/10.3390/su13158274

[2] Vellaiyan, S., Amirthagadeswaran, K.S. (2016). The role of water-in-diesel emulsion and its additives on diesel engine performance and emission levels: A retrospective review. Alexandria Engineering Journal, 55(3): 2463-2472. https://doi.org/10.1016/j.aej.2016.07.021

[3] Abdul Wahhab, H.A., Maskour, M.A., Madodi, S.A. (2020). Investigation of water-diesel emulsion characteristics using optical technique. Journal of Applied Fluid Mechanics, 13(1): 349-355. https://doi.org/10.29252/jafm.13.01.30133

[4] Premalatha, R.P., Parameswari, E., Davamani, V., Malarvizhi, P., Avudainayagam, S. (2019). Biosorption of chromium (III) from aqueous solution by water hyacinth biomass. Madras Agricultural Journal, 106(1-3): 12-21. https://doi.org/10.29321/MAJ 2019.000215

[5] Kalam, A., Rahman, L., Ahmed, N. (2019). Removal of toxic Congo red dye using water hyacinth petiole, an efficient and selective adsorbent. Journal of the Chemical Society of Pakistan, 41(5): 825-833.

[6] Canazart, D.A., Nunes, A.R.D.C., Sanches, M., Conte, H. (2017). Phytoremediation agro industrial wastewater of using macrophyte Eichhornia crassipes. Brazilian Journal of Surgery and Clinical Research, 17(2): 87-91.

[7] Gogoi, P., Adhikari, P., Maji, T.K. (2017). Bioremediation of arsenic from water with citric acid cross-linked water hyacinth (E. crassipes) root powder. Environmental Monitoring and Assessment, 189: 383. https://doi.org/10.1007/s10661-017-6068-2

[8] Nash, D.A.H., Abdullah, S.R.S., Hasan, H.A., Idris, M., Muhammad, N.F., Al-Baldawi, I.A., Ismail, N.I. (2019). Phytoremediation of nutrients and organic carbon from sago mill effluent using water hyacinth (Eichhornia crassipes). Journal of Engineering and Technological Sciences, 51(4): 573-584. https://doi.org/10.5614/j.eng.technol.sci.2019.51.4.8

[9] Sayago, U.F.C. (2019). Design of a sustainable development process between phytoremediation and production of bioethanol with Eichhornia crassipes. Environmental Monitoring and Assessment, 191: 221. https://doi.org/10.1007/s10661-019-7328-0

[10] de Vasconcelos, G.A., Véras, R.M.L., de Lima Silva, J., Cardoso, D.B., de Castro Soares, P., de Morais, N.N.G., Souza, A.C. (2016). Effect of water hyacinth (Eichhornia crassipes) hay inclusion in the diets of sheep. Tropical Animal Health and Production, 48: 539-544. https://doi.org/10.1007/s11250-015-0988-z

[11] Mahmood, S., Khan, N., Iqbal, K.J., Ashraf, M., Khalique, A. (2018). Evaluation of water hyacinth (Eichhornia crassipes) supplemented diets on the growth, digestibility and histology of grass carp (Ctenopharyngodon idella) fingerlings. Journal of Applied Animal Research, 46(1): 24-28. https://doi.org/10.1080/09712119.2016.1256291

[12] Saratale, R.G., Cho, S.-K., Ghodake, G.S., Shin, H.-S., Saratale, G.D., Park, Y., Lee, H.-S., Bharagava, R.N., Kim, D.-S. (2020). Utilization of noxious weed water hyacinth biomass as a potential feedstock for biopolymers production: A novel approach. Polymers, 12(8): 1704. https://doi.org/10.3390/polym12081704

[13] Sundari, M.T., Ramesh, A. (2012). Isolation and characterization of cellulose nanofibers from the aquatic weed water hyacinth - Eichhornia crassipes. Carbohydrate Polymers, 87(2): 1701-1705. https://doi.org/10.1016/j.carbpol.2011.09.076

[14] Setyaningsih, L., Satria, E., Khoironi, H., Dwisari, M., Setyowati, G., Rachmawati, N., Kusuma, R., Anggraeni, J. (2019). Cellulose extracted from water hyacinth and the application in hydrogel. IOP Conference Series:

Materials Science and Engineering, 673: 012017. https://doi.org/10.1088/1757-899X/673/1/012017

[15] Al-Kayiem, H.H., Wahhab, H.A.A., Magaril, E., Aziz, A.R.A. (2018). Performance and emissions investigation of a single cylinder diesel engine using enhanced blend biodiesel by nanoparticles. AIP Conference Proceedings, 2035: 020008. https://doi.org/10.1063/1.5075556

[16] Seela, C.R., Ravi Sankar, B. (2020). Investigations on CI engine with nano-sized zinc oxide added Mahua Methyl Ester blends. International Journal of Ambient Energy, 41(2): 146-151. https://doi.org/10.1080/01430750.2018.1451377

[17] Ashok, B., Nanthagopal, K., Jeevanantham, A.K., Bhowmick, P., Malhotra, D., Agarwal, P. (2017). An assessment of calophyllum inophyllum biodiesel fuelled diesel engine characteristics using novel antioxidant additives. Energy Conversion and Management, 148: 935-943. https://doi.org/10.1016/j.enconman.2017.06.049

[18] Ghafoori, M., Ghobadian, B., Najafi, G., Layeghi, M., Rashidi, A., Mamat, R. (2015). Effect of nano-particles on the performance and emission of a diesel engine using biodiesel-diesel blend. International Journal of Automotive & Mechanical Engineering, 12: 3097-3108. http://doi.org/10.15282/ijame.12.2015.23.0258

[19] Hawi, M., Elwardany, A., Ismail, M., Ahmed, M. (2019). Experimental investigation on performance of a compression ignition engine fueled with waste cooking oil biodiesel–diesel blend enhanced with iron-doped cerium oxide nanoparticles. Energies, 12(5): 798. https://doi.org/10.3390/en12050798

[20] Radhakrishnan, S., Munuswamy, D.B., Devarajan, Y., Mahalingam, A. (2018). Effect of nanoparticle on emission and performance characteristics of a diesel engine fueled with cashew nut shell biodiesel. Energy Sources, Part A: Recovery, Utilization, and Environmental Effects, 40(20): 2485-2493. https://doi.org/10.1080/15567036.2018.1502848

[21] Perumal, V., Ilangkumaran, M. (2018). The influence of copper oxide nano particle added pongamia methyl ester biodiesel on the performance, combustion and emission of a diesel engine. Fuel, 232: 791-802. https://doi.org/10.1016/j.fuel.2018.04.129

[22] Magaril, E., Magaril, R., Al-Kayiem, H.H., Skvortsova, E., Anisimov, I., Rada, E.C. (2019). Investigation on the possibility of increasing the environmental safety and fuel efficiency of vehicles by means of gasoline nano-additive. Sustainability, 11(7): 2165. https://doi.org/10.3390/su11072165

[23] Arockiasamy, P., Anand, R.B. (2015). Performance, combustion and emission characteristics of a DI diesel engine fuelled with nanoparticle blended jatropha biodiesel. Periodica Polytechnica Mechanical Engineering, 59(2): 88-93. https://doi.org/10.3311/PPme.7766

[24] Mayburov, I., Leontyeva, Y. (2015). Transport tax in Russia as a promising tool for the reduction of airborne emissions and the development of the road network. WIT Transactions on Ecology and the Environment, 198: 391-401. https://doi.org/10.2495/AIR150341

[25] Mayburov, I., Leontyeva, Y. (2017). Fiscal instruments for regulating the sustainable development of urban transport systems in Russia. IOP Conference Series: Earth and Environmental Science, 72: 012016. https://doi.org/10.1088/1755-1315/72/1/012016

[26] Fadil, A., Mashkour, M.A., Abdul Wahhab, H.A. (2022). Investment of blending biofuels and nanoparticles with conventional diesel fuel to improve combustion process - A review. Advances in Material Science and Engineering: Selected Articles from ICMMPE 2021, pp. 95-107. https://doi.org/10.1007/978-981-19-3307-3_9

[27] Yaser, H.S., Abdul Wahhab, H.A., Dhahad, H.A. (2022). Survey to water-in-diesel emulsion characteristics as an alternative fuel for CI engine. In Advances in Material Science and Engineering: Selected Articles from ICMMPE 2021, pp. 81-94. https://doi.org/10.1007/978-981-19-3307-3_8

[28] Yaser, H.S., Abdul Wahhab, H.A., Dhahad, H.A. (2022). Influence of water-in-fuel (Diesel and Biodiesel) emulsions on the performance and emission characteristics of a single-cylinder diesel engine. In Advances in Material Science and Engineering: Selected Articles from ICMMPE 2021, pp. 71-79. https://doi.org/10.1007/978-981-19-3307-3_7